

## SOME SIMPLE EQUIVALENT CIRCUITS FOR IONIC CONDUCTORS

J. ROSS MACDONALD and ROBERT L. HURT

*Department of Physics and Astronomy, University of North Carolina, Chapel Hill, NC 27514 (U.S.A.)*

(Received 18th September 1985; in revised form 15th November 1985)

### ABSTRACT

Some equivalent circuits which involve one or two distributed circuit elements are discussed. These circuits are useful in fitting small-signal frequency response data for solids and liquids. A fitting circuit recently proposed by Bruce to represent distributed bulk effects in conducting materials is shown to be closely related to earlier work. Although Bruce demonstrated that his circuit fitted certain data better than a simple alternative circuit, it is not physically realistic in the high frequency region. We investigate how well the response of the Bruce circuit (which involves one distributed circuit element and three ideal elements) can be simulated by that of simpler circuits, ones which involve a single unified distributed element, possibly in parallel with a single ideal capacitor. The usefulness of several different distributed elements, most of which have been widely used for data fitting in the past, is compared. Complex nonlinear least squares fitting results suggest that several of the simpler circuits considered are preferable to the proposed Bruce circuit for fitting of most ionic-conductor frequency response data. Finally, two structurally different equivalent circuits which involve two distributed elements each, so they can represent distributed interface as well as bulk effects, are compared and found to be able to simulate each other quite well under certain conditions. Problems which thus arise in choosing the best equivalent circuit for data fitting are discussed.

### INTRODUCTION

More often than not, the electrical small-signal frequency response of a conductive or dielectric system includes a finite-length frequency range within which the response is proportional to a power,  $n$ , of the angular frequency,  $\omega$ . The exponent  $n$  usually falls in the range  $0 < n < 1$ . When both the real and imaginary parts of an immittance function (impedance, admittance, complex modulus, or complex dielectric constant) depend on frequency in this region with the same exponent  $n$ , the response is that of the constant phase element (CPE), a distributed circuit component whose admittance,  $Y = Y' + iY''$ , may be written [1]

$$Y_{\text{CPE}} = A_0(i\omega)^n = A_0\omega^n [\cos(n\pi/2) + i \sin(n\pi/2)], \quad (1)$$

where  $A_0$  is independent of frequency. Its constant phase angle  $\theta$  is thus just  $n\pi/2$ . Although the CPE is not physically realizable when considered as a response function over all frequencies [1,2], it, or a near approximation to it, is so often found in Impedance Spectroscopy (IS) (for a finite frequency range not including the

extremes of frequency) that such response is almost ubiquitous. This means that when we try to represent IS data by means of an equivalent circuit, it must usually include one or more distributed circuit elements (DCE's) of CPE type or ones which at least exhibit CPE-like response over part of their ranges of applicability.

Although here we shall consider only intrinsically conducting systems, such as ionic hopping conductors, the DCE's we shall use, when expressed in normalized form, are equally applicable to dielectric systems [3]. We shall start by discussing equivalent circuits which involve only a single DCE and shall conclude with a comparison of two circuits involving two DCE's each.

#### EQUIVALENT CIRCUITS INVOLVING A SINGLE DISTRIBUTED ELEMENT

Figures 1a and 1b show two circuits recently compared by Bruce [4] using ionic-conductor IS data and complex nonlinear least squares (CNLS) data fitting [5]. Here  $C_\infty$  is the high frequency limiting capacitance of the system, the geometrical capacitance. It is always properly present in any equivalent circuit and always bridges the electrodes [6,7]. It is often actually omitted from equivalent circuits used to fit data, however, because the data do not extend to sufficiently high frequencies that its effect is apparent. The resistance  $R$  was identified by Bruce only as the dc resistance of the material. Provided that one is working with a material that exhibits only bulk response,  $R$  is also the high frequency limiting bulk resistance of the system,  $R_\infty$ , only equal to the dc resistance when no other resistive contributions appear at lower frequencies [6,7], as is the case here and in Bruce's work [4]. Thus the actual, measured dc resistance is not necessarily the bulk resistance of the system and may even be infinite, but  $R_\infty$  is always present in any real conducting system.

The DCE's in Bruce's circuits were identified only as frequency dependent admittances but were in fact CPE's, as shown in Fig. 1. Although Bruce ascribes the Fig. 1a circuit to a 1977 paper of Jonscher [8], its provenance is actually considerably earlier. The CPE was perhaps first discussed for ionic systems by Fricke [9] in 1932

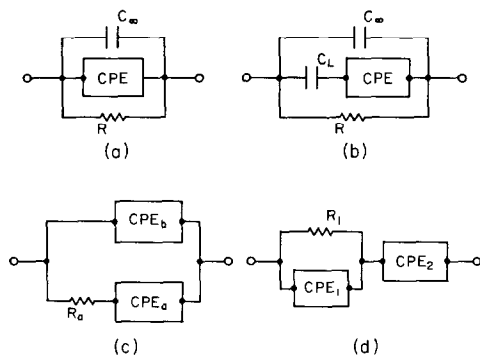


Fig. 1. Four simple equivalent circuits involving constant phase elements (CPE's).

and appears explicitly in the 1941 work of Cole and Cole [10] for dielectric systems. The first (implicit) appearance of the parallel combination of a CPE and a resistor (as in Bruce's Fig. 1a and the present Fig. 1a) in the solid electrolyte area was the introduction by Ravaine and Souquet [11] in 1973 of the distributed impedance function

$$Z = Z' + iZ'' = Y^{-1} = R/[1 + (i\omega\tau_0)^n] \quad (2)$$

which leads, when plotted in the complex plane, to an arc of a circle whose center lies below the real axis for  $0 < n < 1$ . It has thus been termed [3,12] the ZARC DCE. Equation (2) was proposed in analogy to the Cole–Cole (CC) dielectric-system DCE, which has exactly the same functional dependence on frequency at the complex dielectric constant level and thus leads in general to a depressed semicircle in the complex dielectric constant plane [3,10–12].

Although eqn. (2) represents a unitary DCE in its own right and may be interpreted in terms of a distribution of relaxation times in the same way the CC is so interpreted [10], it may also be considered as a composite circuit element, the combination of a CPE and resistor in parallel [1,3,12]. This result follows immediately when we set  $RA_0 = \tau_0^n$ . Although the ZARC has been used to fit considerable data, including some for  $\beta$ -alumina [13], like the CPE it is physically unreasonable at the frequency extremes. Any real linear system with time-invariant material properties should have a shortest (non-zero) relaxation time and a longest (non-infinite) relaxation time [3,12,14]. Thus at sufficiently high and low frequencies the response of a conductive system must reduce to that of a single ideal resistor and capacitor in parallel (no distributed element effects). In turn this requires that as  $\omega \rightarrow 0$ ,  $[1 - (Z'/R)] \propto \omega^2$  and  $-Z'' \propto \omega$ , while for  $\omega \rightarrow \infty$ ,  $Z' \propto \omega^{-2}$  and  $-Z'' \propto \omega^{-1}$ . The ZARC does not satisfy these conditions, which are often of importance only outside the (limited) frequency range of most IS measurements.

The Bruce circuit of Fig. 1b removes one of the frequency-extreme deficiencies of the ZARC and the Fig. 1a circuit, namely the one for  $\omega \rightarrow 0$ . The addition of the capacitor  $C_L$  ensures that the 1b circuit behaves as a capacitor and resistor in parallel in this limit. Incidentally, the series combination of an ideal capacitor and a CPE, as in the Bruce circuit, has been used for many years, since the CC dielectric-system DCE may be considered just such a composite element [3,10]. Bruce was perhaps the first, however, to demonstrate its usefulness for a conductive situation. Now the requirement of RC-type behavior in the frequency extremes necessitates that the arc of an impedance plane plot must intercept the real axis with an angle whose magnitude is  $90^\circ$  at both the low and the high frequency ends. Although this perpendicular-intercept condition has been in the literature for some time [15], it is not well known. It is a necessary but not sufficient condition for physical realizability since it does not ensure limiting single RC behavior. For example, for  $\omega \rightarrow \infty$  the Bruce circuit does lead [4] to a  $90^\circ$  angle (for  $n < 1$ ) but not to high-frequency-limiting RC behavior. Thus this circuit is still not entirely physically reasonable and would require the addition of a new element, a resistor in series with  $C_L$ , to be made physically realistic at both frequency extremes.

Now Bruce has shown that IS data on the molten salt [0.4 Ca(NO<sub>3</sub>)<sub>2</sub> + 0.6 KNO<sub>3</sub>] and on the ionically conducting glass K<sub>2</sub>Si<sub>3</sub>O<sub>7</sub> are appreciably better fitted, using CNLS, by the Fig. 1b circuit than by that of 1a. As may be expected, the improvement occurs principally at lower frequencies where the influence of C<sub>L</sub> is important. Although Bruce shows the comparisons by means of complex impedance plane plots, what he refers to as impedance and plots is actually the complex conjugate impedance,  $Z^* = Z' - iZ''$ . The problem mentioned above with the high frequency limit of the Bruce circuit does not show up clearly on an impedance plane plot. One would require a plot of  $\log(Z')$  vs.  $\log(\omega)$  to distinguish between the Bruce frequency exponent of  $(n - 2)$  and the proper  $-2$  exponent in the  $\omega \rightarrow \infty$  limit.

Now it is of interest to see how well the Bruce circuit can mimic some other equivalent circuits found useful for fitting of IS data. Since most of the circuits to be considered have been used in the past to fit a wide variety of frequency response data, the degree to which the Fig. 1b circuit can simulate the response of these other circuits will yield a measure of its generality and usefulness. Instead of using the Bruce circuit to fit separate "data sets" generated from each of several other circuits involving DCE's, for simplicity we shall reverse the procedure, generate "data" using the Bruce circuit and attempt to fit it with other simple circuits using full CNLS. The data used by Bruce in testing the appropriateness of his circuit were given in their original publication [16] only in the form of complex modulus function graphs for several different temperatures. It is not clear whether the  $Z$  values actually fitted by Bruce were derived by reading points off of these graphs and transforming or not. In order to avoid the errors introduced by such a procedure, but still to maintain a close connection to Bruce's work, we shall generate the "data" to be fitted here using the parameters he obtained for his circuit by CNLS fitting of K<sub>2</sub>Si<sub>3</sub>O<sub>7</sub> data [16]. The temperature associated with these results was not stated by Bruce but appears to be 49.6°C. The parameter values (in specific form) are  $R = 1.266 \times 10^9 \Omega \text{ cm}$ ,  $C_L = 3.249 \times 10^{-12} \text{ F/cm}$ ,  $A_0 = 1.978 \times 10^{-11} \Omega^{-1} \text{ cm}^{-1} \text{ s}^n$ ,  $n = 0.562$ , and  $C_\infty = 7.137 \times 10^{-13} \text{ F/cm}$  (there is a misprint in this last value in ref. 4). Using these values and the Fig. 1b circuit, we generated 51 values of  $Z$  distributed uniformly in log angular frequency in the range  $1 \leq \omega/\text{s}^{-1} \leq 10^5$ .

The circuits fitted to the above "data" all initially consisted of  $C_\infty$  in parallel with a conductive-system unitary DCE. The DCE's used were the ZARC, the Havriliak–Negami [17] (HN), the Williams–Watts [18] (WW), and that following from a distribution of activation energies (DAE) model [3,19], involving a double exponential probability density, the DAE<sub>2</sub>. Only the DAE<sub>2</sub> model, of all those considered in this work, is physically reasonable at both frequency extremes [3]. The empirical HN DCE is of the form

$$Z = R / \left[ 1 + (i\omega\tau_0)^{\psi_1} \right]^{\psi_2} \quad (3)$$

which reduces to the ZARC of eqn. (2) when  $\psi_1 = n$  and  $\psi_2 = 1$ . Exact analytic expressions for the impedances of the other two DCE's are not available, but very accurate approximations for them [3,20] are built into the CNLS fitting routine used here [5]. This routine, which allows many different ideal and DCE's to be used in

TABLE 1

CNLS fitting results of impedance “data” derived from the Bruce circuit with the parameter values shown. The last column shows the results obtained from a fit of the “data” transformed to the complex modulus level. Parameter estimates are shown in the form  $Q/\sigma_r$ , where  $\sigma_r$  is the estimated relative standard deviation of  $Q$

Parameter	Bruce circuit	ZARC	HN	DAE <sub>2</sub>	DAE <sub>2</sub>
$10^{-9}R/\Omega \text{ cm}$	1.266	1.274/ $8 \times 10^{-4}$	1.2706/ $4 \times 10^{-4}$	1.2648/ $2 \times 10^{-4}$	1.2276/ $2.1 \times 10^{-3}$
$10^{11}A_0/\Omega^{-1} \text{ cm}^{-1} \text{ s}^n$	1.978	—	—	—	—
$10^3\tau_0/\text{s}$	1.4146	1.679/ 0.036	2.984/ 0.030	2.092/ $7.6 \times 10^{-4}$	1.959/ $3.3 \times 10^{-3}$
$n, \psi_1, \phi$	0.562	0.7820/ $8.3 \times 10^{-3}$	0.7809/ $3.9 \times 10^{-3}$	1.2103/ $2.6 \times 10^{-3}$	1.3179/ $1.33 \times 10^{-3}$
$\psi_2$	—	—	0.489/ 0.024	—	—
$10^{13}C_L/\text{F cm}^{-1}$	32.49	—	—	—	—
$10^{13}C_\infty/\text{F cm}^{-1}$	7.137	2.83/ 0.14	8.233/ $9.7 \times 10^{-3}$	—	—
$\mathcal{E}_d$	—	—	—	4.048/ 0.016	6.513/ 0.014
$\sigma_f$	—	$3.6 \times 10^6$	$1.59 \times 10^6$	$9.47 \times 10^5$	$1.27 \times 10^{-4}$

many different circuit configurations, is available from one of the authors (J.R.M.).

Fitting results are listed in Table 1 and presented in Figs. 2 and 3. In the tables,  $\sigma_f$  is the estimated standard deviation of the overall fit, and the estimated parameter values,  $Q$ , and their estimated relative standard deviations,  $\sigma_r$ , are shown in the form  $Q/\sigma_r$ . Parameter values shown without a  $\sigma_r$  value were fixed. Unity weighting was employed in the fitting results of Table 1. The parameter values used in the Bruce circuit to generate the “data” fitted are shown in the second column of Table 1. There are two time constants, not involving  $C_\infty$ , which may be calculated for the

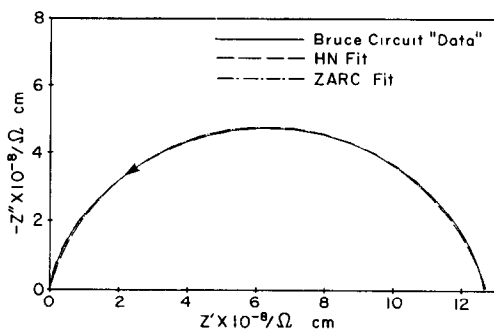


Fig. 2. Complex impedance plane plot comparing “data” calculated from the Bruce circuit with HN and ZARC CNLS fits. As in Table 1,  $C_\infty$  is non-zero here.

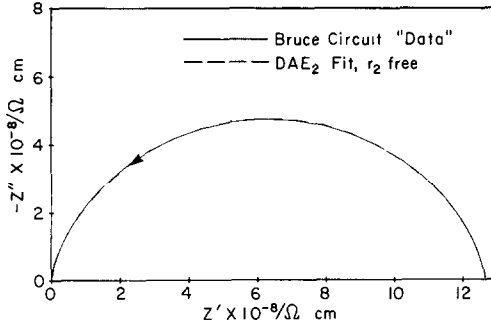


Fig. 3. Complex impedance plane plot comparing the Bruce "data" with the result of a  $DAE_2$  CNLS fit. Here, no extra  $C_\infty$  element was present.

Bruce circuit. The first, which applies at sufficiently low frequencies that the effect of  $C_L$  is dominant, is given by  $\tau_L = (C_L/A_0)^m$ , where  $m = 1/(1-n)$ . It is a CC dielectric-system time constant. The other,  $\tau_0 = (RA_0)^{1/n}$ , is a ZARC conductive-system time constant, dominant when the effects of  $C_L$  are negligible. For the present Bruce parameter values,  $\tau_L = 0.0162$  s, and the value of  $\tau_0$  is given in column two for comparison with the similar time constants of the other DCE's.

The  $DAE_2$  DCE here involves the four parameters  $R$ ,  $\mathcal{E}_d$ ,  $\tau_0$ , and  $\phi$ . Here  $\mathcal{E}_d \equiv \mathcal{E}_1 - \mathcal{E}_0 \equiv 0.5 \ln(r_2)$ , where  $r_2$  is the ratio of the maximum to minimum time constants in the system. In addition,  $\mathcal{E} \equiv E/kT$ ;  $\mathcal{E}_0$  is the lowest normalized activation energy of the system;  $\mathcal{E}_1$  is the central normalized activation energy;  $\mathcal{E}_{\max} = (2\mathcal{E}_1 - \mathcal{E}_0)$  is the maximum normalized activation energy. Although  $\mathcal{E}_0$  may be zero,  $\mathcal{E}_{\max}$  must generally be finite [3]. Since we are dealing with a thermally activated system, it turns out that  $\tau_0$  is of the form  $\tau_0 = \tau_a \exp(\mathcal{E}_1)$ , where we have set the  $\gamma$  of the earlier work [3] equal to unity here and  $\tau_a$  is temperature independent. When  $r_2$  is of the order of  $10^8$  or larger, the complex plane shape following from the model is virtually independent of  $r_2$ , but it does depend on  $r_2$  as  $r_2$  becomes smaller, as is the case here.

It was found that much worse fits were obtained using the  $DAE_2$  in parallel with  $C_\infty$  than without it. For example, the  $\sigma_f$  estimate obtained using the  $DAE_2$  with  $C_\infty$  taken fixed and equal to the Bruce value and with the other parameters free was  $4.67 \times 10^6$ . We found that several DCE's which lead to quite unsymmetric complex plane plots [3] did not yield good fits of the Bruce circuit "data" and their fitting results are therefore not included in Table 1. As Figs. 2 and 3 show, these "data" produce very nearly symmetric impedance plane plots. We do include the potentially asymmetric HN results in Table 1 and in Fig. 2; clearly the actual asymmetry is small here. Not included are the results of WW fitting, which led to a  $\sigma_f$  of about  $3 \times 10^6$ . Here a non-zero  $C_\infty$  of about  $8.7 \times 10^{-13}$  F/cm was quite necessary in order to allow a fairly good fit to be obtained. Incidentally, Boesch and Moynihan [16] (BM) fitted their data only with the WW model, using an approximate approach to do so.

The Table 1 results show that very consistent  $R$  estimates are obtained from all the fits, as well as reasonably consistent  $\tau_0$  estimates. But exponent estimates appear to be quite different. Differences arise in part because  $\phi$  is not quite the same kind of quantity as are  $n$  and  $\psi$ . The possible range of  $\phi$  is  $-\infty < \phi < \infty$ , allowing it to vary linearly with temperature under some conditions [3]. Only when  $\phi \rightarrow \pm \infty$  or  $r_2 \rightarrow 1$  does the DAE<sub>2</sub> lead to single-time-constant Debye response.

Note that the Bruce and HN circuits involve five parameters and the ZARC and DAE<sub>2</sub> only four free parameters, including a  $C_\infty$  parameter in all but the DAE<sub>2</sub> case. Figure 2 shows that even a ZARC fit of actual experimental data like the present Bruce exact “data” could be distinguished from a Bruce-circuit CNLS fit of such data only if the data had very small experimental errors indeed, smaller than typical errors of nearly all real data. The ZARC fit obtained here seems appreciably better than that Bruce obtained with the same fitting circuit. Certainly the HN and DAE<sub>2</sub> fits are so good that they could not be so distinguished unless good data were available which extended far down in the high and/or low frequency tails of the complex plane plots. Although Fig. 3 shows that complex plane graphical distinction between the results of the DAE<sub>2</sub> and the Bruce “data” is impossible over the whole frequency range covered, examination of the numerical fitting residuals showed that deviations increased at the highest frequencies, those where the DAE<sub>2</sub> is physically realistic and the Bruce circuit is not.

The results shown in Table 1 for the ZARC, HN, and the first column of DAE<sub>2</sub> estimates were all obtained from CNLS fitting of the “data” in  $Z$  form, the same level considered by Bruce. But the actual BM data [16] were all given at the  $M$ , or complex modulus level, where  $M \equiv M' + M'' = i\omega C_c Z$ . Here  $C_c$  is the capacitance of the measuring cell when empty. It thus seemed worthwhile to carry out a DAE<sub>2</sub> CNLS fit of the data in  $M$  form for comparison with the  $Z$ -fit results. The last column of Table 1 summarizes the results of such a fit.

In order to transform the  $Z$  data to the  $M$  level, one needs a value of  $C_c$ , a quantity not mentioned by BM or Bruce. Since  $M'(\omega \rightarrow \infty) \equiv M_\infty \equiv C_c/C_\infty$ , however, one can obtain  $C_c$  from knowledge of  $M_\infty$  and  $C_\infty$ . Although BM presented no  $C_\infty$  values, they did list  $M_\infty$  ones. If we therefore combine the BM  $M_\infty = 0.118$  value for their 49.6°C data with the Bruce value of  $C_\infty$ , we obtain  $C_c = 8.422 \times 10^{-14}$  F/cm, the value we employed in the data transformation.

Because of the different effective weighting and magnitudes of data at the  $Z$  and  $M$  levels, one obtains very different  $s_f$  values for  $M$  fits than for  $Z$  fits. If the model were an exact fit to the data, one would, however, obtain exactly the same parameter estimates for either type of fitting. The differences found here are indicative of the effects of systematic errors present in fitting a model to data which are not entirely consistent with the model. Further, the  $M$  transformation weights the higher frequency end of the data set more than the lower end. Incidentally, the  $M$ -level DAE<sub>2</sub> fit was appreciably better at the high frequency end, where relative residuals were less than one percent, than at the low frequency end of the data. Indeed the transformed  $M$  data, and predicted values from the fit, were reasonably close to actual 49.6°C BM data points read off their graphs.

How is it possible that the  $DAE_2$  can yield a very good fit of the Bruce “data”, either at the  $Z$  or the  $M$  level, without a  $C_\infty$  in the fitting circuit? The reason is clear. All the other fitting models, including the Bruce circuit, are physically unrealistic at the high end of the frequency range where the effect of  $C_\infty$  is greatest. They all thus need a  $C_\infty$  in order to allow improved fitting in this region. But the  $DAE_2$  goes to the physically realistic limit of a capacitor and resistor in parallel, in the present conductive-system case, as  $\omega \rightarrow \infty$ . Thus the  $DAE_2$  can well fit data like that of BM, which approaches a constant  $M_\infty$  in the high frequency limit, without the explicit addition of a separate  $C_\infty$  element. A  $C_\infty$  is thus implicitly included in the  $DAE_2$  fit. When, in fact, a separate free  $C_\infty$  parameter is included in the fitting circuit, its value is driven down towards zero during the CNLS fitting process, just as one would expect. Only if experimental or theoretical data were obtained from a model well represented by a resistor in series with a  $DAE_2$  DCE would a separate  $C_\infty$  element be needed. If the original BM data were available, fitting with such an element and a series resistor would be warranted. Note that one of the virtues of CNLS fitting is that the addition of possible redundant circuit elements in the equivalent circuit being fit does no harm. If an element is redundant, its final estimated value will either be negligible compared to the effects of other circuit elements and/or its relative standard deviation will be of the order of unity or greater. Such elements can then be eliminated from the circuit used for a final fitting.

For comparison with the  $M$ -level  $DAE_2$  fit, we also carried out a ZARC plus  $C_\infty$  fit at the  $M$  level. The fit was appreciably better, relative to that of the  $DAE_2$ , at the  $M$  level as compared to that at the  $Z$  level. For example, a value of  $\sigma_f$  of  $1.32 \times 10^{-4}$  was found, much closer to that of the  $DAE_2$  at this level. Further, the estimated  $C_\infty$  value found and its estimated relative standard deviation were  $6.95 \times 10^{-13} / 2 \times 10^{-3}$  F/cm, much closer to the actual Bruce value used in generating the data.

Although the present fitting results are not completely comparable to those of Bruce using the Fig. 1a and 1b circuits, they show that the ZARC and a parallel capacitor can simulate the Bruce circuit much better than Bruce concluded. The origin of the difference is unknown. In any event, it appears that the ZARC, or even better, the HN, with a parallel  $C_\infty$  can simulate the Bruce circuit more than adequately in almost all practical cases; both circuits also require the same or fewer parameters and are simpler in form than Bruce’s circuit. Thus Bruce’s claims for the special usefulness of his circuit and his identification of a particular physical process modelled by  $C_L$  seem somewhat nugatory.

It is quite clear that the original data [16] are associated with a thermally activated system; further they also involve a distribution of relaxation times (DRT), not just a single-time-constant Debye response. It is thus plausible to assume that the DRT arises from a DAE and that the  $DAE_2$  model is therefore particularly appropriate for analyzing the data. Certainly it can fit the present Bruce “data” very well indeed with only four parameters, as opposed to five for the non-thermally-activated Bruce circuit, and it may well be the most appropriate model for the original BM experimental data as well.



## EQUIVALENT CIRCUITS INVOLVING TWO DISTRIBUTED ELEMENTS

Thus far we have dealt with a situation where some or all of the bulk properties of the material are distributed and have paid no attention to interface effects. But most ionically conducting materials with highly conducting electrodes do exhibit such effects, particularly when the frequency range is extended to very low frequencies. Further, it is often more likely that interface properties are distributed than that bulk ones are, especially for homogeneous materials and single crystals. Just as distributed bulk properties lead to the need for one or more DCE's in a fitting equivalent circuit, so too do distributed interface properties. Therefore, it is not unreasonable to expect to find that two or more DCE's are needed to fit experimental data that cover an appreciable frequency range, particularly one extending to low frequencies. Here we shall compare two such circuits, omitting  $C_\infty$  elements for simplicity.

The circuit of Fig. 1c has been used by Bates [21] to fit some of his recent data on single-crystal  $\beta$ -alumina at room temperature and below. That of Fig. 1d has also been used to fit [22] earlier data [13] on this material. Note that it is essentially just the Fig. 1a circuit with a CPE in series with it to represent interface effects. Bates was kind enough to send us some of his new data, along with fitting results for  $T = 150$  K for the Fig. 1c circuit. It was thus natural for us to try fitting these data with the Fig. 1d circuit. We were initially quite surprised to obtain parameter estimates nearly identical to those obtained from Bates' fitting. To investigate these results more systematically, we used the parameter estimates obtained from fitting to generate new Fig. 1c "data". These data involved 89 impedance values covering the range from 100 to  $7 \times 10^5$  Hz in equal logarithmic steps. Because of the wide range of impedance magnitude covered by the data, for the CNLS fitting we used weighting derived by assuming that the uncertainty in a real or imaginary data value was proportional to its magnitude.

Results of our various fits are summarized in Tables 2 and 3. The first column shows the parameter values from which the data were generated and the second shows the results of CNLS fitting to the 1d circuit. All CPE "A" parameter values correspond to the  $A_0$  parameter of eqn. (1). As mentioned above, very close

TABLE 2

Circuit transformation fitting results in the form  $Q/\sigma_r$ , where  $\sigma_r$  is the estimated relative standard deviation of  $Q$

Circuit Fig. 1c	Circuit Fig. 1d	Circuit Fig. 1c
$R_a = 1.3 \times 10^5$	$R_1 = 1.26 \times 10^5 / 2.6 \times 10^{-4}$	$R_a = 1.300 \times 10^5 / 2.7 \times 10^{-4}$
$A_a = 3.5 \times 10^{-9}$	$A_2 = 3.537 \times 10^{-9} / 5.8 \times 10^{-4}$	$A_a = 1.864 \times 10^{-8} / 4.9 \times 10^{-4}$
$n_a = 0.91$	$n_2 = 0.9103 / 7.1 \times 10^{-5}$	$n_a = 0.9100 / 7.2 \times 10^{-5}$
$A_b = 3.5 \times 10^{-11}$	$A_1 = 3.73 \times 10^{-11} / 3.7 \times 10^{-3}$	$A_b = 2.046 \times 10^{-10} / 3.4 \times 10^{-3}$
$n_b = 0.96$	$n_1 = 0.9569 / 2.98 \times 10^{-4}$	$n_b = 0.9599 / 3.2 \times 10^{-4}$
$\sigma_f = -$	$\sigma_f = 1.26 \times 10^{-3}$	$\sigma_f = 1.24 \times 10^{-3}$

TABLE 3

Circuit transformation fitting results

Circuit Fig. 1c	Circuit Fig. 1d	Circuit Fig. 1c
$R_a = 1.3 \times 10^5$	$R_1 = 3.29 \times 10^2 / 8.3 \times 10^{-3}$	$R_a = 2.088 \times 10^5 / 9.4 \times 10^{-3}$
$A_a = 10^{-10}$	$A_2 = 1.097 \times 10^{-9} / 4.2 \times 10^{-4}$	$A_a = 2.44 \times 10^{-10} / 1.7 \times 10^{-2}$
$n_a = 0.91$	$n_2 = 0.9565 / 2.4 \times 10^{-5}$	$n_a = 0.9612 / 1.3 \times 10^{-3}$
$A_b = 10^{-9}$	$A_1 = 2.31 \times 10^{-8} / 3.3 \times 10^{-2}$	$A_b = 6.12 \times 10^{-9} / 7.2 \times 10^{-4}$
$n_b = 0.96$	$n_1 = 0.9647 / 2.6 \times 10^{-3}$	$n_b = 0.9563 / 5.8 \times 10^{-5}$
$\sigma_f = -$	$\sigma_f = 1.75 \times 10^{-3}$	$\sigma_f = 6.1 \times 10^{-4}$

agreement is obtained for the Table 2 values. Note especially that the interface DCE of the Fig. 1d circuit,  $CPE_2$ , corresponds to the CPE in series with  $R_a$  in Fig. 1c,  $CPE_a$ , as might be expected. When this identification is appropriate,  $CPE_b$  describes distributed bulk effects in Fig. 1c. The two circuits then become identical when no interface element is present.

It was also of interest to examine how well the reverse transformation worked. Thus we used the parameter estimates of the middle column to generate "data" from the Fig. 1d circuit and fitted these data using the Fig. 1c circuit. With perfect fits one would expect to recover the exact column 1 parameter values. Comparison of the column two and three values of Table II shows that the corresponding CPE  $A$  values are appreciably less close to each other than are those of columns 1 and 2. Finally, comparison of the column 3 results with those of column 1 indicates the degree to which systematic errors distort the fitting results. Clearly, we can estimate CPE  $n$  exponent values here appreciably better than  $A$  ones, and only little weight should be given to the absolute values of estimated  $\sigma_f$  values in situations where appreciable systematic errors are present. Figure 4 shows a complex plane log-log plot of the original Fig. 1c impedance data and the 1d fitting results. Even in the Fig. 5 linear complex plane plot (of part of the data only) little or no difference between original and fitted values can be discerned. Nevertheless, the above comparison shows that even for such an excellent fit we are unable to return very closely to the original  $A$  parameter values. Since the above conclusions are often not well recognized, they need to be emphasized.

Table 3 summarizes similar fitting results, but ones where we have appreciably changed the ratio of the two input  $A$  parameters as compared to the Table 2 situation. Here interface effects are relatively more important over the frequency range covered (a smaller value of the  $A$  parameter leads to a larger value of the series interface impedance magnitude). Further, the values shown in columns two and three agree much less well than those found for the Table 2 results. Particularly interesting is the  $R$  value of column two which is about 400 times smaller than that of column one. We see that although both circuits can fit data of the present type more or less equally well, they can predict very different bulk resistance values. If we did not know in advance which circuit was most appropriate for given data, we

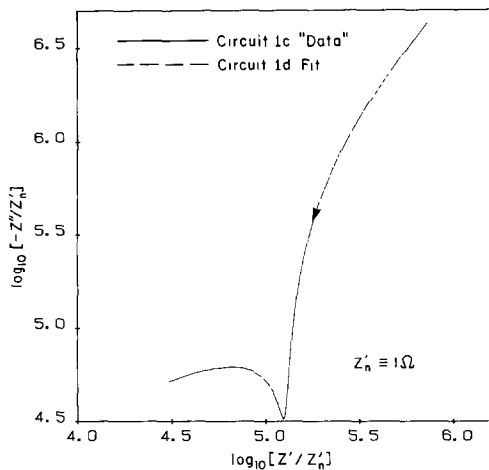


Fig. 4. Complex impedance plane plot, with logarithmic scales, of "data" associated with columns one (circuit of Fig. 1c, —) and two (CNLS fit using circuit of Fig. 1d, - - -) of Table 2

could end up with a wildly inappropriate  $R$  estimate by fitting with the wrong circuit. Again, as shown by the log-log complex plane plot of Fig. 6, the CNLS fit is so good here that one cannot distinguish graphically between the original data and the predicted impedance values, even though they are associated with different fitting circuits involving appreciably different parameter values. Clearly, additional information beyond goodness of fit is needed in cases such as these to allow a proper choice of fitting circuit to be made.

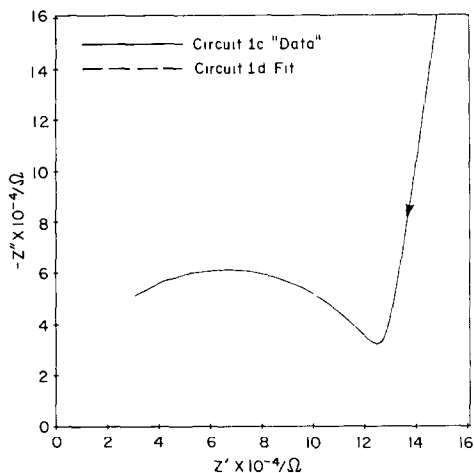


Fig. 5. Complex impedance plane plot, with linear scales, of "data" associated with columns one (circuit of Fig. 1c, —) and two (CNLS fit using circuit of Fig. 1d, - - -) of Table 2.

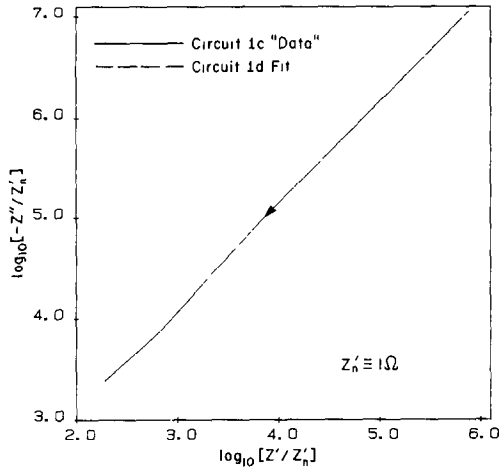


Fig. 6. Complex impedance plane plot, with logarithmic scales, of "data" associated with columns one (circuit of Fig. 1c, —) and two (CNLS fit using circuit of Fig. 1d, - - -) of Table 3.

The close agreement of the results of columns one and two of Table 2 and even the appreciable differences in the corresponding values of Table 3 can be explained in the following way. It will have been noted that for the present Bates type of data the values of  $n_a$  and  $n_b$  are close to unity, making the CPE's approximate ideal capacitors. Consider circuits like those of Fig. 1c and 1d where the CPE's are indeed replaced by capacitors with the same subscripts. Thus  $A_a \rightarrow C_a$  and so on. Then with the proper relations between the parameters of the two circuits, they may be made to exhibit the same impedance at all frequencies [6,7]. The relations are

$$\begin{aligned} R_1 &= R_a \delta^2 & R_a &= R_1 \Delta^{-2} \\ C_1 &= C_b / \delta & C_a &= C_2 \Delta \\ C_2 &= C_a + C_b & C_b &= C_1 \Delta \end{aligned}$$

and

$$C_1 + C_2 = \delta^{-2} C_a$$

where

$$\delta \equiv C_a / (C_a + C_b) \quad \text{and} \quad \Delta \equiv C_2 / (C_1 + C_2)$$

Now because the  $n$ 's are all close to unity for the results of Tables 2 and 3, the above equations still hold approximately when the  $C$ 's are replaced by  $A$ 's, as may be readily verified using the present parameter values. For example, the predicted  $R_1$  of Table 3 is about 1074, and the  $R_a$  of column 3 is about  $1.6 \times 10^5$ . But such approximate relationships between the parameters of the two DCE circuits naturally become less and less accurate as the  $n$  values decrease from unity. A consequence is that the Fig. 1c and 1d circuits are able to simulate each other, by being able to fit

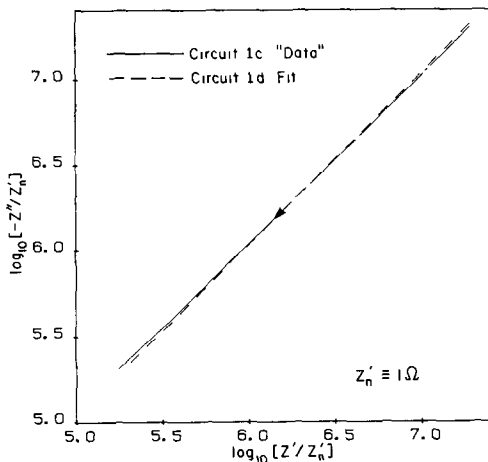


Fig. 7. Complex impedance plane plot, with logarithmic scales, of "data" derived from most of the parameters of Table 2, column one, but with  $n_a = 0.5$  and  $n_b = 0.8$  (circuit of Fig. 1c, —), and from fitting these data with the circuit of Fig. 1d (---)

data derived from the other, worse and worse as the  $n$ 's decrease. Thus, for example, if the  $n_a$  and  $n_b$  values of column one of Table 2 are changed to 0.5 and 0.8, respectively, or to 0.4 and 0.7, respectively, and all other values kept the same, the  $\sigma_f$  values found from fitting with the Fig. 1d circuit are 0.021 and 0.051, much worse fits than obtained with the larger  $n$ 's. Actual log-log complex plane comparison for the first choice above appears in Fig. 7.

The results of Bruce and of the present work suggest that when an equivalent circuit which contains one or more CPE's, rather than other more physically realistic DCE's, is to be used in attempting to find a good fitting circuit, one should usually try comparing the efficacy of the circuit containing ordinary CPE's with the same circuit with capacitors in series with some or all of the CPE's. When CNLS fitting is employed, as it should be, any useless parameters can be readily identified, by comparison of  $\sigma_f$  estimates, and eliminated on the next fit. On the other hand, the present results also suggest that there will usually be a superior alternative to using fitting circuits involving non-physical CPE's.

The search for an appropriate equivalent circuit to fit experimental IS data should always include CNLS fitting with several different circuits in order to determine the best fitting one. When the circuits tried include one or more DCE's, one of the selected circuits will usually yield an appreciably better fit than the others. If it is physically reasonable as well, it should be selected. But if two or more circuits yield comparable fits, either because of the ambiguities discussed above or possibly because of the presence of appreciable errors in the data, other information is needed to allow the best choice to be made. For example, one could repeat the experiment for several different temperatures and/or electrode separations. That

circuit which led to the least, or the most plausible, dependence of the parameters on these variables would then be the most appropriate.

#### ACKNOWLEDGEMENTS

We acknowledge with thanks data received from Dr. John Bates, and the support of this work by the U.S. Army Research Office.

#### REFERENCES

- 1 J.R. Macdonald, *Solid State Ionics*, 13 (1984) 147.
- 2 J.R. Macdonald and M.K. Brachman, *Rev. Mod. Phys.*, 28 (1956) 393.
- 3 J.R. Macdonald, *J. Appl. Phys.*, 58 (1985) 1955, 1971.
- 4 P.G. Bruce, *J. Electroanal. Chem.*, 181 (1984) 289.
- 5 J.R. Macdonald, J. Schoonman and A.P. Lehn, *J. Electroanal. Chem.*, 131 (1982) 77
- 6 J.R. Macdonald, *J. Electroanal. Chem.*, 40 (1972) 440.
- 7 D.R. Franceschetti and J.R. Macdonald, *J. Electroanal. Chem.*, 82 (1977) 271. See Fig. 5.
- 8 A.K. Jonscher, *Nature*, 279 (1977) 673.
- 9 H. Fricke, *Philos. Mag.*, 14 (1932) 310
- 10 K.S. Cole and R.H. Cole, *J. Chem. Phys.*, 9 (1941) 341.
- 11 D. Ravaine and J.-L. Souquet, *C.R. Acad. Sci. (Paris)*, 277C (1973) 489.
- 12 J.R. Macdonald, *Solid State Ionics*, 15 (1985) 159.
- 13 D.P. Almond and A.R. West, *Solid State Ionics*, 9/10 (1983) 277; 11 (1983) 57.
- 14 J.R. Macdonald, *J. Appl. Phys.*, 34 (1963) 538.
- 15 R. Syed, D.L. Gavin, C.T. Moynihan and A.V. Lesikar, *J. Am. Ceram. Soc.*, 64 (1981) 118C.
- 16 L.P. Boesch and C.T. Moynihan, *J. Non-Cryst. Solids*, 17 (1975) 44.
- 17 S. Havriliak and S. Negami, *J. Polymer Sci.*, C14 (1966) 99.
- 18 G. Williams and D.C. Watts, *Trans. Faraday Soc.*, 66 (1970) 80.
- 19 J.R. Macdonald, *Phys. Rev. B*, submitted.
- 20 J.R. Macdonald and R.L. Hurt, *J. Chem. Phys.*, 84 (1986) 496.
- 21 J.R. Bates, private communication, 1984.
- 22 J.R. Macdonald and G.B. Cook, *J. Electroanal. Chem.*, 168 (1984) 335; 193 (1985) 57.